Indian Journal of Chemistry
Vol. 63, February 2024, pp. 176-180
DOI: 10.56042/ijc.v63i2.5075

Theoretical investigation on interacting zones of certain flavones

Sivaranjani G, Vanitha K & Sadasivam K*

Department of Physics, Bannari Amman Institute of Technology, Sathyamangalam 638 401, Tamil Nadu, India

E-mail: dftsada@gmail.com

Received 23 August 2023; accepted (revised) 25 January 2024

Quantitative molecular electrostatic potential (MESP) analysis is performed to delineate the reactive sites of the six plant secondary metabolites from the flavone family. Reactive sites are visualized and interpreted through the MESP descriptors (A_+, A_-, σ_+^2, σ_-^2, υ, $\upsilon\sigma_{Tot}^2$ and MPI) which reveals the accepting and donating propensity of H-bond. In addition, the most negative potential $V_{min}(r)$ is obtained by the presence of delocalized π-electrons or lone pair of electrons in the compounds, as the result of increasing electron density. Also, partial positive charges generated near the H-atoms in the compounds will increase the magnitude of most positive potential $V_{max}(r)$. Density functional theory (DFT) tool is employed to elucidate the MESP for apigenin (**CA**), scutellarein (**CB**), chrysoeriol (**CC**), hispidulin (**CD**), myricetin (**CE**) and mearnsetin (**CF**). Depending on these considerations, active reactive site of the chosen compounds is explored.

Keywords: Molecular polarity index, Electrostatic potential, Electrophilic region, Nucleophilic region, Degree of balance

Molecular electrostatic potential (MESP) illustrate the distribution of charges where excess of electron and deficiency of electron are interpreted visually with the aid of three dimensional surfaces. The molecular reactivity is evaluated with respect to the reactive zones comprising of electrophilic (electron-donating) and nucleophilic (electron-withdrawing) sites. Non-covalent interactions among the atoms are predicted *via* MESP analysis was initiated by Scrocco and Tomasi[1]. Certain color codes are utilized to categorize the negative potential (represented in red color) and positive potential (depicted in blue color). Further, the extrema of positive potential is visualized through small orange sphere whereas negative potential is explored through tiny cyan sphere. Electrostatic potential (V(r)) is evaluated by the following relation (1):

$$V(r) = \sum_{\alpha=1}^{M} \frac{Z_\alpha}{|R_\alpha - r|} - \frac{\rho(r')d^3r'}{|r-r'|} \quad \ldots(1)$$

where, Z_α contributes the nuclear charge at R_α, ρ is the electron density, negative V(r) provide electron density and presence of positive charge is exhibited by V(r). In addition to that $V_{max}(r)$ and $V_{min}(r)$ represents existences of electropositive and electronegative atoms at the specified sites[2].

Also, the electrostatic interactions are examined through the MESP descriptors including positive surface area A_+, negative surface area A_-, positive variance σ_+^2, negative variance σ_-^2, degree of balance υ, product of degree of balance with total variance $\upsilon\sigma_{Tot}^2$ and molecular polarity index MPI. Propensity of interaction of the system with the electrophilic species is observed by the following relations (2) and (3) for σ_+^2 and σ_-^2.

$$\sigma_+^2 = \frac{1}{m}\sum_{i=1}^{m} V^+(r_i) - \overline{V_{max}^+(r_i)}^{\,2} \quad \ldots(2)$$

$$\sigma_-^2 = \frac{1}{n}\sum_{j=1}^{n} \left[V^-(r_j) - \overline{V_{min}^-(r_i)}\right]^2 \quad \ldots(3)$$

where, $\overline{V_{max}^+(r_i)}$ and $\overline{V_{min}^-(r_i)}$ are the average values of positive and negative potential respectively[3, 4].

Degree of balance, $\upsilon = \sigma_+^2\sigma_-^2 \Big/ \sigma_{Tot}^2$, where, σ_{Tot}^2 is the total variance, $\sigma_{Tot}^2 = \sigma_+^2 + \sigma_-^2$. When the value of υ closely approaches 0.25, either it would be a weaker or stronger interaction. The strongest electrostatic potential of the surface can be explored by the term $\upsilon\sigma_{Tot}^2$, which is the product of degree of balance (υ) and total variance (σ_{Tot}^2)[5]. The term molecular polarity index (MPI) expound the polarity of the system *via* the electrostatic potential and it is calculated by the pursuant relation (4)[6-9].

$$MPI = \frac{1}{A}\int_S |V(r)|\, dS \quad \ldots(4)$$

where, A is the surface area of the system.

The present work is focused to explore on the intermolecular interactions of naturally occurring flavonoid compounds such as apigenin (4',5,7-trihydroxyflavone), scutellarein (4',5,6,7-tetrahydroxyflavone), chrysoeriol (4',5,7-trihydroxy-3'-methoxyflavone), hispidulin (4',5,7-trihydroxy-6-methoxyflavone), myricetin (3,5,7,3',4',5'-hexahydroxyflavone) and mearnsetin (3,5,7,3',5'-pentahydroxy-4'-methoxyflavone)[10-12] which are represented in Fig. 1. These compounds are well known for certain biological activities among them few are anti-inflammatory agents, antineoplastic agents, antioxidant agent, anticonvulsant, antiproliferative and antimetastatic activities.

Theoretical methodology

Using exchange – correlation functional in DFT, geometrical optimization is performed through the global hybrid functional (M06-2X) combined with 6-311 G (d,p) basis set. Gaussian 16W software package is employed in gas phase for optimizing the chosen metabolites. Quantitative MESP is generated with the aid of Multiwfn 3.8 analyzer program[13] and all isosurfaces of the all compounds are constructed through visual molecular dynamics (VMD) software.

Results and Discussion

The isosurfaces of all the chosen secondary metabolites are plotted and depicted in Fig. 2. The electrophilic interaction is observed near the O-4 position in C ring due to the presence of maximum negative potential for the **CA** as represented in Fig. 2a and Table 1. Further, presence of sea of electrons is also observed at O-4 position due to the fact that population of unpaired electrons is more at that position. Conversely, the repulsive potential nature is witnessed at 4' OH position in B ring because of cluster of positive charges gathered at that point

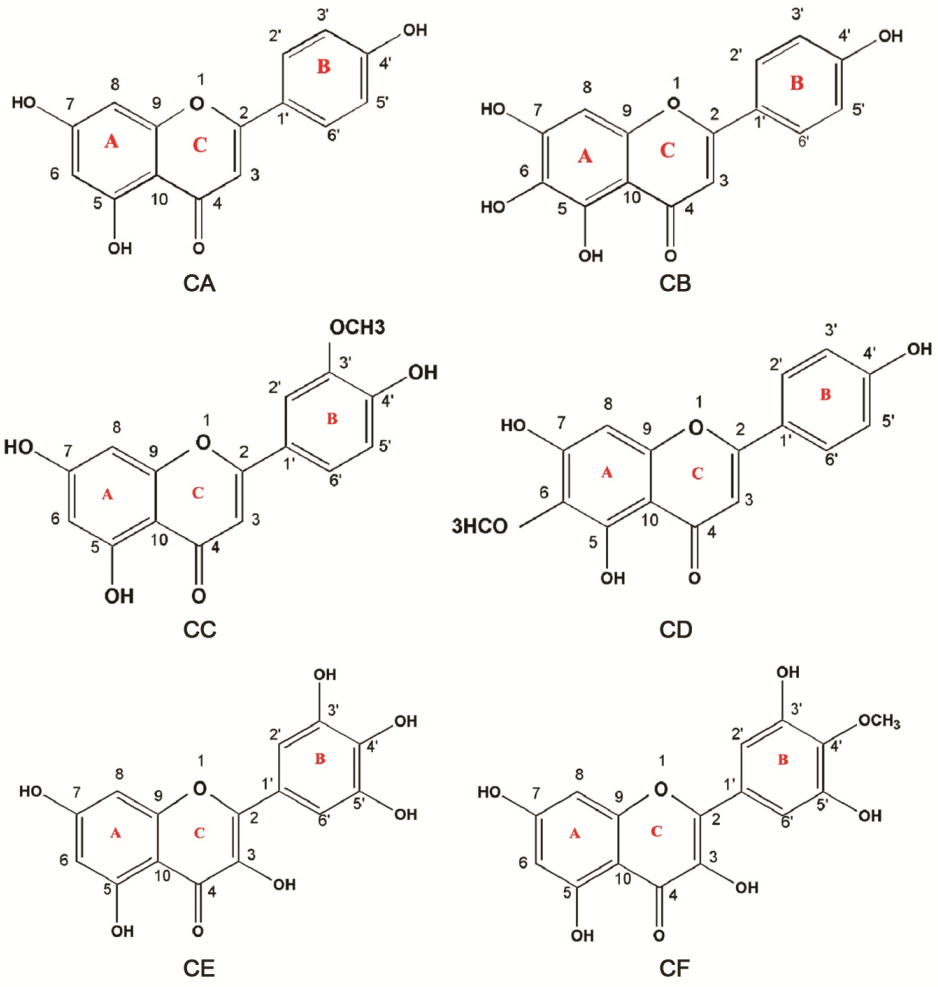

Fig. 1 — Chemical structure of the chosen compounds (**CA** – **CF**).

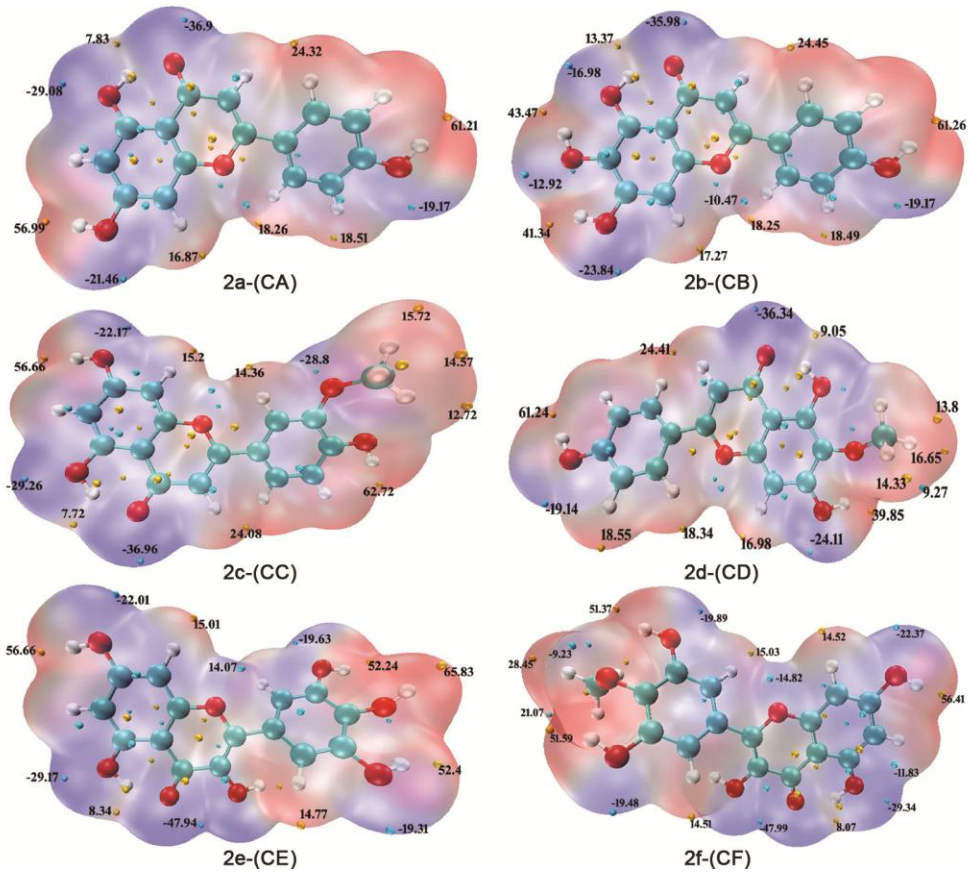

Fig. 2 — 2a, 2b, 2c, 2d, 2e and 2f are the isosurface of all chosen flavone family.

Table 1 — Descriptors of MESP including most positive potential ($V_{max}(r)$), most negative potential ($V_{min}(r)$), positive surface area (A_+), negative surface area (A_-), positive variance ($\boldsymbol{\sigma_+^2}$), negative variance ($\boldsymbol{\sigma_-^2}$), total variance ($\boldsymbol{\sigma_{Tot}^2}$), degree of balance ($\upsilon$), the product of degree of charge balance with total variance ($\upsilon\boldsymbol{\sigma_{Tot}^2}$) and molecular polarity index (MPI) are computed and interpreted

MESP descriptors	Compd					
	A	**B**	**C**	**D**	**E**	**F**
$V_{max}(r)$ (kcal/mol)	61.21	61.24	62.71	61.16	65.81	56.45
$V_{min}(r)$ (kcal/mol)	–36.9	–35.97	–36.96	–36.34	–47.88	–47.97
A_+ (Å^2)	117.24	117.71	137.01	139.22	128.38	144.07
A_- (Å^2)	159.68	165.56	168.78	164.83	170.22	174.24
$\boldsymbol{\sigma_+^2}$ ((kcal/mol)^2)	182.11	154.89	167.45	122.68	268.38	153.7
$\boldsymbol{\sigma_-^2}$ ((kcal/mol)^2)	69.97	55.92	75.71	70.54	104.53	102.44
$\boldsymbol{\sigma_{Tot}^2}$ ((kcal/mol)^2)	252.08	210.81	243.17	193.22	372.91	256.14
υ	0.20	0.19	0.21	0.23	0.20	0.24
$\upsilon\boldsymbol{\sigma_{Tot}^2}$ ((kcal/mol)^2)	50.5	41.1	52.1	44.7	75.22	61.47
MPI (kcal/mol)	12.32	11.17	12.49	11.43	14.26	13.98

which in turn exhibit nucleophilic interactions. The magnitude of electrophilic region is higher due to the delocalization of electrons of the O-atom than nucleophilic region in both the positive and negative surfaces. This clearly reveal that the **CA** readily interact with the electrophilic region due to higher positive variance σ_+^2. The degree of balance of **CA** is about 0.20 in which the balance between the σ_+^2 and σ_-^2 expound the presence of interactions (strong or weak) in both positive and negative regions. Strongest interaction is observed in the **CA** by the magnitude of 50.5 $(kcal/mol)^2$. Due to higher MPI (electronegative atom), the compound possesses stronger polarity[2, 14, 15]. It is found that the 4' OH region of **CA** is capable of donating a positive charge and acts as best antioxidant from the magnitude of $V_{max}(r)$ which is in good agreement with BDE magnitudes[16].

The isosurface of **CB** is depicted in Fig. 2b, in which, the electrophilic site is observed near the oxygen atom in C ring and this is due to the maximum magnitude of $V_{min}(r)$. High negative potential indicates greater electron density where attractive potential is exhibited over the region. Concurrently, the magnitude of $V_{max}(r)$ is obtained at the 4' – OH group and it is preferential site for nucleophilic attack. This site is a dominating repulsive potential zone as a result of presence of cluster of positive charges in that region. The value of electrophilic zone is greater than nucleophilic zone because of the presence of delocalized π – electron. The magnitude of σ_+^2 is larger than σ_-^2, reveals that **CB** possess electrophilic nature. The balance of σ_+^2 and σ_-^2 (υ=*0.19*) indicates that the **CB** interact through both the positive and negative regions and bespeaks about either strong or weak interactions. Strong interaction is explored by the magnitude obtained by $\nu\sigma_{Tot}^2$. Due to the larger MPI, the stronger polarity of **CB** is observed from Table 1. Therefore, the compound CB has the ability for the transfer of proton from the 4' OH site which is quantitatively established by BDE magnitudes[17,18]. Fig. 2c depicts the MESP surface of **CC** in which the electrophilic interacting region is witnessed at O – atom in C ring and this implies that this region consists of high electron density. Also this site possess attractive potential due to lone pair of electrons and π-electrons present in the 4-O atom. Similarly, nucleophilic interaction region is found near 4' OH and this is the impact of positive charges in the region indicates repulsive nature of potential. Further the delocalization of electrons is observed at O-atom. **CC** is featured to interact with the electrophilic region due to the maximum value of positive variance. Above all the **CC** possess strong interaction as well as exhibiting intense polarity (Table 1). Nucleophilic potential is observed at 4' OH zone due to the existence of sea of positive charges and deprotonation is more facile at the particular zone. Like **CB**, in **CC** also the 4' OH site is the best zone for the radical scavenging and the same is revealed by BDE values already reported[11]. As delineated in Fig. 2d, in **CD** most negative potential $V_{min}(r)$ is found at O-atom in which the density of electron is higher, thus the region is preferred for electrophilic interaction while the site 4' OH is the preferential site for nucleophilic interaction where the positive charge density is higher. Hence this surface is more prone to both attractive (O-atom) and repulsive (4' OH) potentials. In this compound, the negative surface area is higher than the positive surface area because of the presence of a lone pair of electron at the O atom in the C ring (Table 1). σ_+^2 describes the interacting nature with respect to electrophilic site within **CD**. The $\nu\sigma_{Tot}^2$ and MPI reveals that the **CD** possesses strong electrostatic interaction as well as the strong polarity. The zone 4' OH have high density of positive charges which indicates the ability to donate a positive charge and the reported BDE[11] reveals that **CD** is the best radical scavenger.

Quantitative MESP surface of **CE** is illustrated in Fig. 2e where the attractive potential is observed at 4-O atom of C ring. This is due to the presence of lone pair of electron which may cause high electron density. The 4' OH site exhibit repulsive characteristics because of low density of electrons where nucleophilic attack is possible. The delocalized π – electron zone is established through negative surface area (170.22 $Å^2$) which is greater than the positive surface area (128.38 $Å^2$). Strong electrostatic potential and strong polarity are observed in **CE** as depicted in Table 1. Even though the 4-O atom possesses high electron density it is unable to release an electron due to the steric hindrance afford by the formation of H bond. Therefore, the 4' OH site is the most favorable site for the neutralization of the radical compared to the remaining OH sites subsequently revealed by the previously published data[19].

Electrophilic and nucleophilic interaction positions are illustrated in Fig. 2f for the **CF**. The 4 – O and 3 – OH positions of C ring are highly prone to

electrophilic attack whereas 7-OH in B ring exhibits nucleophilic attack. Delocalized electron in oxygen atom would rise the magnitude of electrophilic region (A_-) rather than the nucleophilic region (A_+). The σ_+^2 delineate the interacting ability with the electrophilic site within the compound. Based on the degree of balance this compound has strong interacting nature (Table 1). Probability of donating a charge is found to be more facile at 7 OH in B ring where the magnitude of nucleophilic potential comparatively larger due to the gathering of positive charges over the region.

Conclusion

In this article, features of MESP with respect to scavenging activity for a cluster of flavones are simulated and interpreted. Through MESP analysis, the favorable site for radical scavenging behavior of chosen flavones are explored quantitatively. These compounds exhibit negative and positive potentials due to the presence of both the charges on the surfaces which are identified *via* MESP descriptors. Among the six chosen flavones, the $V_{max}(r)$, $\upsilon\ \sigma_{Tot}^2$ and MPI of **CE** is found to be maximum which shows the strong polarity as well as strong interaction nature. Based on these factors all the six flavones are ordered as follows.

$V_{max}(r)$: **CE** > **CC** > **CB** > **CA** > **CD** > **CF**

$\upsilon\sigma_{Tot}^2$: **CE** > **CF** > **CC** > **CA** > **CD** > **CB**

MPI : **CE** > **CF** > **CC** > **CA** > **CD** > **CB**

The entire MESP analysis delineate that the compound **CE** (myricetin) is observed to be a best radical scavenger.

Conflict of interest

On the behalf of all authors Sadasivam K declares that there is no conflict of interest either in terms of financial commitment or review process.

Acknowledgments

The authors are thankful to Bannari Amman Institute of Technology for the necessary infrastructural facilities provided to carry out the research.

References

1 Alaminsky R J & Seminario J M, *J Mol Model.,* 25 (2019) 160.
2 Kenouche S, Sandoval-Yañez C & Martínez-Araya J I, *Chem Phys Lett,* 801 (2022) 139708.
3 Liu Z, Lu T & Chen Q, *Carbon,* 171 (2021) 514.
4 Murray J S, Brinck T, Lane P, Paulsen K & Politzer P, *J Mol Struct,* 307 (1994) 55.
5 Politzer P & Murray J S, *Theor Chem Acc,* 108 (2002) 134.
6 Zhang M & Zhu X, *Comp Theor Chem,* 1190 (2020) 113005.
7 Murray J S & Politzer P, *Theor Chem Acc,* 425 (1998) 107.
8 Bouhmaida N & Ghermani N E, *J Phys Chem,* 122 (2005) 114101.
9 Politzer P, Murray J S & Flodmark P, *J Phys Chem,* 100 (1996) 5538.
10 Sadasivam K & Kumaresan R, *Mol Phys,* 109 (2011) 839.
11 Sadasivam K & Kumaresan R, *Comp Theor Chem,* 963 (2011) 227.
12 Sadasivam K & Kumaresan R, *Spectrochim Acta A,* 79 (2011) 282.
13 Tian L & Feiwu C, *J Comp Chem,* 33 (2011) 580.
14 Murray J S, Lane P, Brinck T & Politzer P, *J Phys Chem,* 97 (1993) 5144.
15 Chen L, Panpan C, Cunlei L & Jingang W, *Catalysts,* 12 (2022) 561.
16 Messaadiaa L, Bekkar Y, Benamira M & Lahmar H, *Chem Phys*, 1 (2020) 100007.
17 Spiegel M, Marino T, Prejanò M & Russo N, *J Mol Liq,* 366 (2022) 120343.
18 Spiegel M, Marino T, Prejanò M & Russo N, *Antioxidants,* 11 (2022) 224.
19 Ali H M & Ali I H, *Med Chem Res*, 28 (2019) 2262.